

This is an Accepted Manuscript version of the following article, accepted for publication in:

J. del Olmo, J. Poza, L. Aldasoro, T. Nieva and G. Ugalde, "Automatic detection test of current sensor faults for induction motor drives at standstill," 2016 XXII International Conference on Electrical Machines (ICEM), 2016, pp. 2178-2183.

DOI: <https://doi.org/10.1109/ICELMACH.2016.7732824>

© 2016 IEEE. Personal use of this material is permitted. Permission from IEEE must be obtained for all other uses, in any current or future media, including reprinting/republishing this material for advertising or promotional purposes, creating new collective works, for resale or redistribution to servers or lists, or reuse of any copyrighted component of this work in other works.

# Automatic detection test of current sensor faults for induction motor drives at standstill

Jon del Olmo\*, Javier Poza\*, Leire Aldasoro\*\*, Txomin Nieva\*\*, Gaizka Ugalde\*

**Abstract** – This paper proposes an automatic detection test of gain faults in current sensors. An offline test is applied when the machine is not operating. The designed test operates at standstill without being necessary to disconnect the machine from the application. Current sensors are part of a commercial induction motor drive composed by a bilevel inverter, an induction motor and an electronic control unit. Therefore, in the selection of the approach, memory usage, computational cost and real-time implementation have been carefully considered. The algorithm, based on the model of the motor, uses the parameter  $\sigma L_s$  of the machine as a fault indicator. In order to estimate that parameter, firstly, precalculated width voltage pulses are injected into the motor using the inverter. Secondly the generated current slope is measured. Finally the estimation is compared to its nominal value. Once the theoretical basis is explained, the execution sequence of the test and the simulation results are presented. In addition, some enhancements are proposed to improve the resolution and accuracy of the approach, because the real conditions of the test do not follow exactly some of the theoretical assumptions.

**Index Terms**—Automatic, current sensor, fault detection, induction motor drive, standstill test, transient inductance, parameter estimation.

## I. NOMENCLATURE

|                        |                                                    |
|------------------------|----------------------------------------------------|
| RAMS                   | Reliability, Availability, Maintainability, Safety |
| FDI                    | Fault Detection and Identification                 |
| DSP                    | Digital Signal Processor                           |
| IPMSM                  | Interior Permanent Magnet Synchronous Machine      |
| $\widehat{\sigma L_s}$ | Measured transient inductance                      |
| $\Delta i$             | Theoretical current difference                     |
| $\widehat{\Delta i}$   | Measured current difference                        |
| $\tilde{G}_{est}$      | Estimated sensor gain error                        |
| $\tilde{G}_{fault}$    | Estimated sensor gain error due to sensor fault    |
| $\tilde{G}_{test}$     | Estimated sensor gain error due to test inaccuracy |

## II. INTRODUCTION

Reliability, availability, maintainability and safety (RAMS) are getting more and more attention in the field of electric drives. These concepts must be taken into account from the conception stage. It is not enough to consider only cost and dynamic behaviour criteria; safety and availability requirements must also be fulfilled. Once it is verified that the system meets several safety standards, which is considered essential, availability can be enhanced by:

- Improving the reliability of the system, designing it to minimise faults, choosing more robust components and architectures.

- Making maintenance procedures easier and faster while the equipment is out of operation during maintenance.

Fig. 1 shows a generic variable speed induction motor drive. Among the elements of the system, sensors are considered to be the weak link due to their key role in control and supervision tasks [1]–[2]. On the one hand, they provide the information to close the loop for the control strategy. On the other hand, they are a key component of the supervision and protection subsystem.

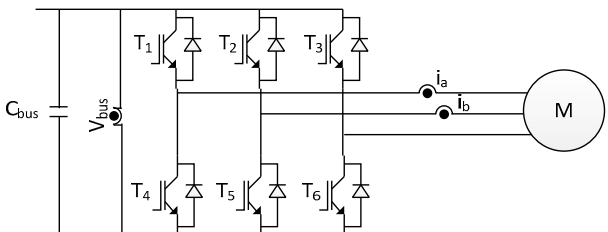


Fig. 1 Generic electric drive

When a sensor fails, it usually causes a complete shutdown of the system, because the control algorithm is not able to continue working without measurements. Even if the control strategy is robust enough to keep the electric drive working in some sort of degraded mode, faulty sensors cause false alarms and abnormal behaviours, which create safety issues [3].

This paper addresses the problem of validating phase current sensor measurements in electric drives. Although nowadays electric drive designs tend to minimise the number of current sensors, most of them include at least two, due to the lack of models that calculate motor variables with only one current sensor [4]. Hence, it is crucial to validate the health of this kind of devices.

In the field of sensor fault detection and diagnostics, several strategies have been developed over the last decades. These strategies use either physical redundancy or analytical redundancy. Physical redundancy means that more sensors than those needed for the control strategy are installed. In this way, two or more measurements of the same variable can be compared to find anomalies, and the faulty device can be replaced by the healthy extra sensor. In any case, this strategy is commonly discarded, since it increases the weight, cost and size of the drive [5]–[7]. Analytical redundancy strategies, where the needed extra information is analytically calculated, include state observers, parity equations, Kalman filters and parameter identification.

State observer theory has been widely used in current sensor fault detection and identification. Observers are closed-loop algorithms that combine measurements and analytical models to estimate the state variables of the observed system. Then, those estimations can be compared

\*University of Mondragon, Faculty of Engineering, 20500 Mondragón, Spain. (e-mail: jdelolmo@mondragon.edu; jpoza@mondragon.edu; gugalde@mondragon.edu).

\*\*CAF Power and Automation, Polígono Katategi, 20271 Irura, Spain. (laldasoro@cafpower.com;tneiva@cafpower.com)

with actual measurements to detect any mismatch. Rothenhagen and Fuchs [9]–[11] studied the use of state observers to identify current sensor faults in doubly-fed induction generators. They developed a fault detection and reconfiguration scheme based on a bank of observers capable of detecting and isolating current sensor faults and assuring fault tolerant control. In the same way, Grouz et al. [12] present a bank of observers for PMSM machines. In [13], Najafabadi et al. propose a full order adaptive Lyapunov-based observer that avoids the use of a bank and takes into account the variation of the rotor resistance in an induction-motor drive.

Parity equations have also been used in the field of current sensor FDI. This theory transforms conventional state-space models in order to get residuals that enhance fault isolation [14]. The approach has been used to detect current sensor faults in IPMSM drives [15] and in induction machine drives [16]. Berirri et al. present in [17] a parity space based strategy that focuses in real-time applications. They argue that the real-time implementation of most model-based strategies is too complex. Hence, they focus on developing a new algorithm that minimises the use of sensor output readings and it is insensitive to parameter variations.

Even though it is not the most common approach, Kalman filtering technique has also been applied to sensor FDI in electric drives. The work presented in [18] uses a three phase signal model combined with Kalman Filters to detect current sensor faults. The authors claim that they can avoid uncertainties introduced by the variation of model parameters using a signal model instead of a motor model.

Finally it is worth mentioning that some researchers have tried developing parameter identification techniques to detect several faults. Parameters such as stator and rotor resistances have been used as motor health indicators in [19] and [20]. Others have combined model-based methods with parameter identification techniques to avoid false alarms and make model-based approaches adaptive [13][21].

Nevertheless, in the field of current sensor fault detection, parameter identification techniques have not yet been investigated as a standalone alternative to the aforementioned methodologies. Therefore, in this paper a strategy to validate motor current sensors using the estimation of the  $\sigma L_s$  transient inductance parameter as a health indicator is proposed. The test will be used in a commercial electric drive where the characteristics of the inverter and the motor are known.

In applications like railways or aeronautics, maintenance is carried out in depots, where the electric drive has limited functionalities. In this scenario, standstill parameter identification techniques can be very helpful, since they do not need to rotate the motor in order to perform the estimation. This is the case of the test presented here, which estimates the transient inductance ( $\sigma L_s$ ) and detects sensor gain faults using single phase voltage supply, without the need to rotate the machine. Moreover, the strategy proposed in this paper tries to deal with the limitations of a real-time implementation in a commercial DSP-based Electronic Control Unit. This means that issues such as memory usage,

algorithm complexity and computational cost had to be taken into account. Due to these constraints, a parameter identification technique was selected, ruling out any closed loop or observer based approaches.

The paper is organised as follows. Section III deals with the model of the induction motor, the estimation of the transient inductance and the limitations of the approach. Section IV redefines the estimation algorithm for sensor fault detection purposes. Section V presents simulation results and section VI draws conclusions.

### III. TRANSIENT INDUCTANCE ESTIMATION

#### A. Theoretical approximation of the transient inductance

As described in [22], the estimation of the transient inductance of an induction machine can be achieved applying short voltage pulses to the stator, by means of an inverter, and measuring the slope of the stator current in one phase. Such sequence can be seen in Fig. 2.

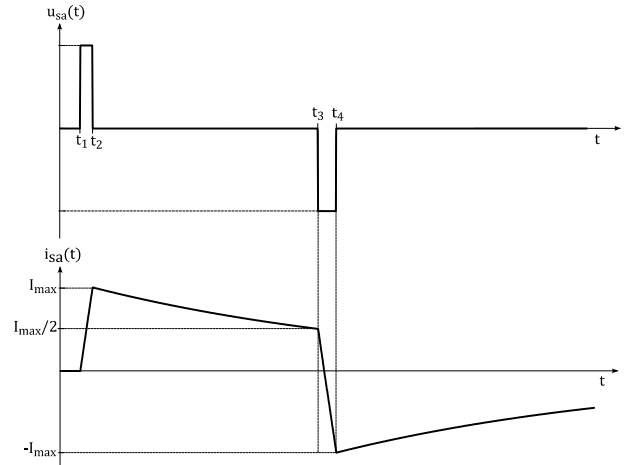


Fig. 2 Evolution of stator voltage pulses and generated current

For this purpose, the induction machine is described by its model in the  $\alpha$ - $\beta$  stationary reference frame, where the stator voltage vector  $\vec{u}_s$ , the stator current vector  $\vec{i}_s$  and the magnetizing current vector  $\vec{i}_{mr}$  are the state variables:

$$\vec{u}_s = R_s \vec{i}_s + \frac{d\vec{\Psi}_s}{dt} \quad (1)$$

$$\vec{\Psi}_s = L_s \vec{i}_s + L_h \vec{i}_{mr} \quad (2)$$

$$\vec{i}_{mr} = \frac{L_r}{L_h} \vec{i}_r + \vec{i}_s = \frac{\vec{\Psi}_r}{L_h} \quad (3)$$

Combining (1) and (2), the stator voltage is given as a function of the stator and rotor currents:

$$\vec{u}_s = R_s \vec{i}_s + L_s \frac{d\vec{i}_s}{dt} + L_h \frac{d\vec{i}_r}{dt} \quad (4)$$

Replacing  $\vec{i}_r$  from (3) into (4), one obtains:

$$\begin{aligned} \vec{u}_s &= R_s \vec{i}_s + \sigma L_s \frac{d\vec{i}_s}{dt} + (1 - \sigma) L_s \frac{d\vec{i}_{mr}}{dt} \\ \sigma &= 1 - \frac{L_h^2}{L_s L_r} \end{aligned} \quad (5)$$

The equation of the rotor voltage in the stationary

reference frame is:

$$0 = \vec{i}_s - \vec{i}_{mr} - \tau_r \frac{d\vec{i}_{mr}}{dt} + \omega_m \tau_r \vec{i}_{mr} \quad (6)$$

As it was mentioned before, the test proposed here will be at  $\omega_m = 0$ , hence, (6) can be rewritten as:

$$\frac{d\vec{i}_{mr}}{dt} = \frac{\vec{i}_s - \vec{i}_{mr}}{\tau_r} \quad (7)$$

The derivative of the magnetizing current appears in equation (5). Combining (5) and (7) the stator voltage as a function of  $\vec{i}_s$  and  $\vec{i}_{mr}$  is obtained.

$$\vec{u}_s = R_s \vec{i}_s + \sigma L_s \frac{d\vec{i}_s}{dt} + (1 - \sigma) L_s \frac{\vec{i}_s - \vec{i}_{mr}}{\tau_r} \quad (8)$$

Rearranging (8)  $\vec{u}_s$  can be expressed as:

$$\begin{aligned} \vec{u}_s &= R_{rs} \vec{i}_s + \sigma L_s \frac{d\vec{i}_s}{dt} - \frac{L_h^2}{L_r^2} R_r \vec{i}_{mr} \\ R_{rs} &= R_s + L_h^2 \cdot \frac{R_r}{L_r^2} \end{aligned} \quad (9)$$

Substituting (3) into (9) the stator voltage vector can be defined as a function of the stator current and rotor flux vectors:

$$\vec{u}_s = R_{rs} \vec{i}_s + \sigma L_s \frac{d\vec{i}_s}{dt} - \frac{L_h}{L_r} \frac{\Psi_{ar}}{\tau_r} \quad (10)$$

Using equation (10), the behaviour of the induction machine during the  $\sigma L_s$  estimation test can be analysed. The stator voltage in  $a$  axis is:

$$u_{as} = \sigma L_s \frac{di_{as}}{dt} + R_{rs} i_{as} - \frac{L_h}{L_r} \frac{\Psi_{ar}}{\tau_r} \quad (11)$$

If voltage pulses are short enough, it can be assumed that the last two terms of expression (11) are negligible with respect to the current derivative. Therefore,  $\sigma L_s$  can be defined as:

$$\sigma L_s = \frac{u_s}{\frac{di_{as}}{dt}} \quad (12)$$

Equation (12) is used to estimate the value of  $\sigma L_s$ , measuring the applied voltage and the generated current slope.

If an inverter fed electric motor is available, the amplitude of the constant voltage pulses is defined by the voltage vectors generated by the inverter. Depending on the phase it is being monitored, certain vector must be applied. TABLE I shows the selected vectors.

TABLE I  
VOLTAGE VECTORS TO BE APPLIED IN THE ESTIMATION TEST

| Vector         | T <sub>1</sub> | T <sub>2</sub> | T <sub>3</sub> | u <sub>sa</sub>       | u <sub>sb</sub>       |
|----------------|----------------|----------------|----------------|-----------------------|-----------------------|
| V <sub>0</sub> | 0              | 0              | 0              | 0                     | 0                     |
| V <sub>2</sub> | 0              | 1              | 0              | -V <sub>bus</sub> /3  | 2V <sub>bus</sub> /3  |
| V <sub>3</sub> | 0              | 1              | 1              | -2V <sub>bus</sub> /3 | V <sub>bus</sub> /3   |
| V <sub>4</sub> | 1              | 0              | 0              | 2V <sub>bus</sub> /3  | -V <sub>bus</sub> /3  |
| V <sub>5</sub> | 1              | 0              | 1              | V <sub>bus</sub> /3   | -2V <sub>bus</sub> /3 |

The first voltage pulse is applied at instant t<sub>1</sub>, with  $u_{sa} = 2/3V_{bus}$ . The current starts increasing and the pulse is

supplied until the current reaches the maximum value specified for the test ( $i_{as}(t_2) = I_{max}$ ). At t<sub>2</sub>, motor terminals are short-circuited and the stator currents start to decrease. At instant t<sub>3</sub>, when the current falls off to more or less half of  $I_{max}$ , a negative voltage is applied and the current decreases to the minimum ( $i_{as}(t_4) = -I_{max}$ ). The stator terminals are short-circuited again and the current starts to rise.

The  $\frac{di_{as}}{dt}$  in equation (12) is equivalent to the slope of the stator current in the interval  $t_1 - t_2$  or  $t_3 - t_4$ . Since  $t_3 - t_4 > t_1 - t_2$ , the estimation will be more accurate if it is performed between t<sub>3</sub> and t<sub>4</sub>. Using the definition of the slope,  $\sigma L_s$  can be estimated as:

$$\widehat{\sigma L_s} = -\frac{2}{3} \cdot V_{bus} \cdot \frac{t_4 - t_3}{i_{as}(t_4) - i_{as}(t_3)} \quad (13)$$

### B. Limitations of the approximation

Depending on the magnitude of parameter  $\sigma L_s$  and the accuracy requirements for the test, the assumptions made to obtain (13) may not be acceptable.

Firstly, it must be taken into account that in (13) the slope of the current is assumed to be constant (see Fig. 3).

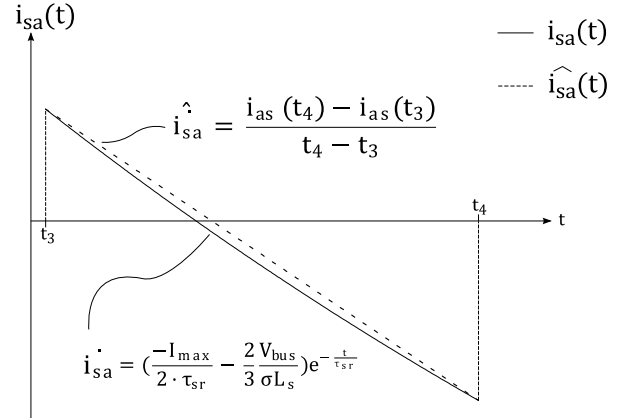


Fig. 3 Comparison of the estimated current curve and real curve

Returning to the analytical expression of the stator voltage in (11), the real slope or derivative that the current will have between t<sub>3</sub> and t<sub>4</sub> can be calculated. Considering that  $i_{as}(t_3) = \frac{I_{max}}{2}$  and  $u_{as}(t_3) = \frac{-2V_{bus}}{3}$ , the derivative is:

$$\frac{di_{as}}{dt} \approx \left( \frac{-I_{max}}{2\tau_{sr}} - \frac{2V_{bus}}{3\sigma L_s} \right) e^{-\frac{t}{\tau_{sr}}} \quad (14)$$

where  $\tau_{sr} = \sigma L_s / R_{sr}$ . Hence, one of the limitations for the estimation could be the approximation of the curve to a line.

Secondly, another issue to bear in mind is the effect of the resistance term in (11), since its value with respect to the value of the derivative increases as the time goes by. It means that the longer the pulses are, the bigger the estimation error is, because the term  $R_{rs} i_{as}$  is not negligible anymore.

Finally, it should be mentioned that the resistance of the motor depends on the temperature, which could also affect to the result of the test.

Such limitations will be taken into account in the implementation of the test, so as to minimise the estimation error and increase the accuracy of the algorithm.

## IV. ESTIMATION TEST FOR SENSOR VALIDATION PURPOSES

### A. Procedure

If the test described in the previous section is intended for current sensor validation purposes, voltage pulses cannot be applied following the evolution of the current, as it was mentioned before. The main problem is that time instants are measured when the current reaches certain values, which is not reliable if the current measurements are inaccurate.

As an alternative to this approach, the application of precalculated width pulses is proposed. The length of the pulses is calculated theoretically assuming the current levels in Fig. 2. Using the analytical approximation for the current response in intervals  $t_1 - t_2$ ,  $t_2 - t_3$  y  $t_3 - t_4$ , such response can be described as:

$$i_a(t) = \begin{cases} I_0(1 - e^{-\frac{t-t_1}{\tau_{sr}}}) & t_1 < t < t_2 \\ I_{max} \cdot e^{-\frac{t-t_2}{\tau_{sr}}} & t_2 < t < t_3 \\ -I_0 + \left(\frac{I_{max}}{2} + I_0\right) e^{-\frac{t-t_3}{\tau_{sr}}} & t_3 < t < t_4 \end{cases} \quad (15)$$

where  $\tau_{sr} = \frac{L_s \sigma}{R_{sr}}$  and  $I_0 = \frac{2 V_{bus}}{3 R_{sr}}$ .

The expressions showed in (15) have been obtained solving the differential equation (11), with the initial conditions for each interval and  $\Psi_r = 0$ . In this way, the time instants, taking  $t_1$  as the initial point are:

$$\begin{aligned} t_2 &= -\tau_{sr} \ln\left(-\frac{I_{max}}{I_0} + 1\right) + t_1 \\ t_3 &= \ln(2) \cdot \tau_{sr} + t_2 \\ t_4 &= -\tau_{sr} \ln\left(\frac{-I_{max} + I_0}{\frac{I_{max}}{2} + I_0}\right) + t_3 \end{aligned} \quad (16)$$

Considering this, the validation process of phase current sensors with the transient inductance estimation is presented in Fig. 4. It is assumed that before the execution of the test, other faults such as current sensor offsets, bus voltage sensor faults and semiconductor faults have been ruled out.

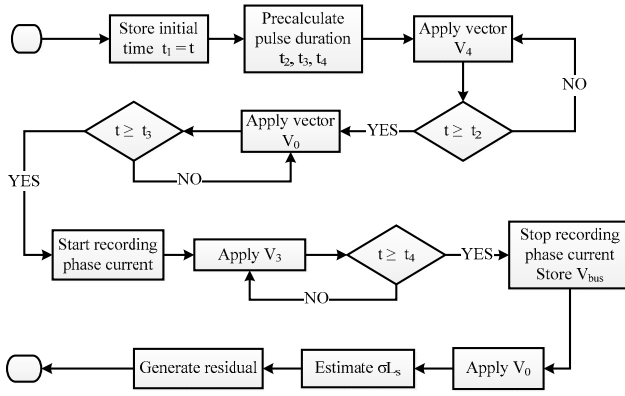


Fig. 4 Test execution sequence for phase a

### B. Residual generation

The basic residual that is generated to validate the measurement is the difference between the estimated and the theoretical parameter:

$$r = \widehat{\sigma L_s} - \sigma L_s \quad (17)$$

Anyway, it must be mentioned that if the test is used to validate phase current sensors, it is quite useful to calculate the deviation between the measured and the theoretical current difference:

$$r_i = \widehat{\Delta i} - \Delta i = (i_{as}(t_4) - i_{as}(t_3)) - \frac{2}{3} V_{bus} \frac{t_4 - t_3}{\sigma L_s} \quad (18)$$

The theoretical  $\sigma L_s$  value is obtained during the control strategy calibration process.

## V. SIMULATION RESULTS

Simulations were performed in Matlab/Simulink to check the validity of the proposed test. The motor used in those simulations has the following characteristics:

| TABLE II<br>INDUCTION MOTOR CHARACTERISTICS |          |
|---------------------------------------------|----------|
| Parameter                                   | Value    |
| Nominal power                               | 54 kW    |
| Nominal speed                               | 1439 rpm |
| Maximum torque                              | 359 Nm   |
| Pole pairs                                  | 2        |
| Line rms voltage                            | 448 V    |
| Nominal rms current                         | 136 A    |
| Stator resistance (20°C)                    | 23.5 mΩ  |
| Rotor resistance (20°C)                     | 24 mΩ    |
| Stator inductance                           | 11.62 mH |
| Rotor inductance                            | 11.52 mH |
| Magnetizing inductance                      | 11.2 mH  |

### A. Basic test simulations

The sequence shown in Fig. 4 has been implemented in a Matlab/Simulink script together with the model of the motor. The main parameters of the test are shown in TABLE III. In Fig. 5 the applied voltage and the current in phase a can be seen.

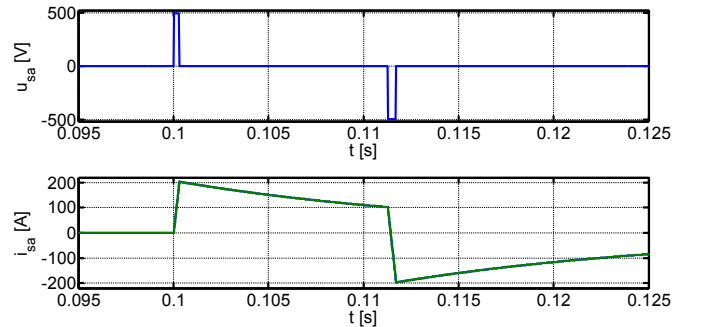


Fig. 5 Evolution of the stator voltage and current in phase a

TABLE III  
SIMULATION PARAMETERS

| Test execution period          | 20 μs      |
|--------------------------------|------------|
| t <sub>1</sub>                 | 100 ms     |
| t <sub>2</sub> -t <sub>1</sub> | 295.179 μs |
| t <sub>3</sub> -t <sub>2</sub> | 10.972 ms  |
| t <sub>4</sub> -t <sub>3</sub> | 440.730 μs |
| V <sub>bus</sub>               | 750 V      |
| I <sub>max</sub>               | 200 A      |

It is worth mentioning that the test for both phases could be performed in less than 500 ms, taking into consideration the time values presented in TABLE III and Fig. 5, and that the current should return to zero before the second phase is

tested. TABLE IV introduces the results of the test with different motor temperatures. For the sake of simplicity, temperature is considered equal in the stator and in the rotor. As it can be seen, the algorithm estimates the parameter with a 0.39% error with respect to the theoretical value at 20°C. The error increases to 0.86% at 120°C. Using the current residual, in the worst case the error reaches 2.47 A (following equation (18)). It means that the test will not be able to detect current deviations smaller than 2.47 A.

TABLE IV  
 $\sigma L_s$  ESTIMATION RESULTS

| Temperature | $\sigma L_s$<br>[ $\mu\text{H}$ ] | $\widehat{\sigma L}_s$<br>[ $\mu\text{H}$ ] | r<br>[%] | $r_i$<br>[A] |
|-------------|-----------------------------------|---------------------------------------------|----------|--------------|
| 20°C        | 73.1111                           | 73.4035                                     | 0.39     | 1.14         |
| 120 °C      |                                   | 73.7465                                     | 0.86     | 2.47         |

### B. Enhanced test

In order to improve the accuracy of the estimation, the use of more current samples in  $t_3 - t_4$  is proposed. With intermediate samples, the current can be interpolated as a line using the least squares method. In that way the current derivative approximation error can be minimised and therefore, the  $\sigma L_s$  estimation error is decreased.

Fig. 6 shows the measured current, the initial approximation with two samples ( $i_{as}(t_3)$  and  $i_{as}(t_4)$ ) and the least squares method approximation with intermediate samples.

Thanks to the least squares method, the error between the samples and the curve is reduced with respect to the initial approximation. TABLE V gathers the results of the enhanced test.

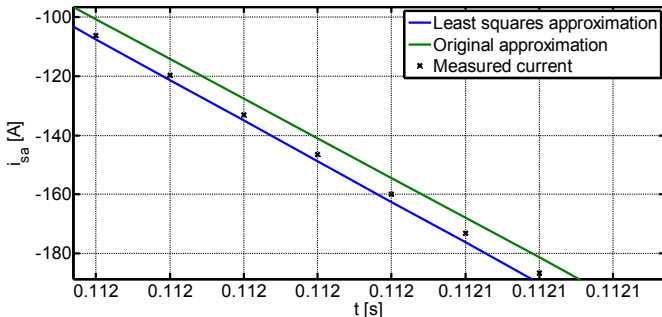


Fig. 6 Current samples and approximation curves

TABLE V  
 $\sigma L_s$  ESTIMATION RESULTS WITH ENHANCED TEST

| Temperature | $\sigma L_s$<br>[ $\mu\text{H}$ ] | $\widehat{\sigma L}_s$<br>[ $\mu\text{H}$ ] | r<br>[%] | $r_i$<br>[A] |
|-------------|-----------------------------------|---------------------------------------------|----------|--------------|
| 20°C        | 73.1111                           | 73.1272                                     | 0.02     | 0.06         |
| 120 °C      |                                   | 73.3617                                     | 0.34     | 0.98         |

Comparing the results from TABLE IV and TABLE V the improvement in the estimation can be seen. Another benefit of using the least squares method is that it makes the test more immune to measurement noise and digitalisation errors.

Finally, another phenomenon that should be taken into account in the analysis of the intrinsic error of the test is the machine saturation. The levels of the voltage pulses and their duration are selected during the calibration process. Once these are set, the test always applies the same current profile for the same machine. Hence, if there is any saturation effect it will affect equally every time. It can be taken as a constant

and intrinsic error of the test and can be compensated in the algorithm.

### C. Sensor gain fault detection

From the current sensor validation point of view, sensor faults up to  $\pm 50\%$  in its gain have been simulated. As it was demonstrated before, the test itself makes an estimation error. Equation (19) shows the relationship between the estimated and the theoretical current, where  $\tilde{G}_{fault}$  is the gain error introduced by the sensor fault,  $\tilde{G}_{test}$  is the gain error introduced by the test and  $\tilde{G}_{est}$  is the total gain error:

$$\Delta i = \Delta i \left( 1 + \frac{\tilde{G}_{est}}{100} \right) = \Delta i \left( 1 + \frac{\tilde{G}_{fault} + \tilde{G}_{test}}{100} \right) \quad (19)$$

Fig. 7 presents the relationship between the total gain error and the gain error introduced by the test, at different temperatures.

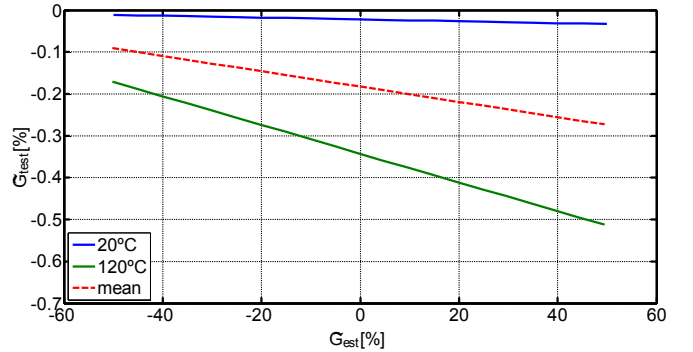


Fig. 7 Gain error due to test with respect to total gain error

$\tilde{G}_{test}$  increases with temperature and with the total gain error. The main effect of the temperature is the variation of the motor resistance. If the electric drive's control includes some sort of resistance estimation strategy as a protection, that estimation could be used to tune the test and get more accuracy.

If such estimation is not available, the use of a mean test gain error curve as a function of the total gain error is proposed (see Fig. 7). The gain error due to the test could be calculated as:

$$\tilde{G}_{fault} = \tilde{G}_{est} - f(\tilde{G}_{est}) = (1 + 0.0018)\tilde{G}_{est} + 0.1819 \quad (20)$$

With this function, the gain error due to the fault can be estimated with a maximum error of  $\pm 0.5\%$ , in a range of 20°C-120°C. It is considered that this error is small enough to perform an effective detection of current sensor faults. It should be taken into account that the rest of elements in the current acquisition sequence (input filters, conditioning stages, quantization,...) could introduce bigger errors than the test itself.

## VI. CONCLUSIONS

This paper has presented an automatic procedure to detect and assess gain faults in current sensors, analysing the dynamic behaviour of an induction motor supplied by voltage pulses. In this way, the need to use external voltage sources and measurement equipment is avoided. The test, based on the motor model, can estimate the deviation of the current measurements with a  $\pm 0.5\%$  error, being insensitive to temperature changes in a range from 20°C to 120°C. With

regard to the time needed to perform the test, it could be executed in less than 500 ms for two sensors. Considering the level of accuracy, the execution duration and the non-invasive characteristics of the test in terms of external equipment, this test is recommended for industrial induction drives. In such devices, the test could be performed by an Intelligent Maintenance System on demand.

## VII. ACKNOWLEDGMENTS

This work has been partially supported by the programs: Universidad Empresa (UE-2014-09) and Formación de Investigadores del Departamento de Educación, Universidades e Investigación from the Basque Government.

## VIII. REFERENCES

- [1] T. Achour and M. Pietrzak-David, "Service continuity of an IM distributed railway traction with a speed sensor fault," in *European Conference on Power Electronics and Applications (EPE)*, 2011, pp. 1–8.
- [2] M. Abdellatif, "Continuité de service des entraînements électriques pour une machine à induction alimentée par le stator et le rotor en présence de défauts capteurs," L'Ecole Nationale d'Ingenieurs de Tunis, 2010.
- [3] G. Betta and A. Pietrosanto, "Instrument fault detection and isolation: State of the art and new research trends," *IEEE Trans. Instrum. Meas.*, vol. 49, no. 1, pp. 100–107, 2000.
- [4] R. Aranz, A. Mendoza, L. J. Miguel, and J. R. Peran, "Sensor and inverter fault tolerant control in induction motors," *IFAC Fault Detect. Superv. Saf. Tech. Process.*, vol. 6, no. 1, pp. 920–925, 2006.
- [5] I. Samy, I. Postlethwaite, and D.-W. Gu, "Survey and application of sensor fault detection and isolation schemes," *Control Eng. Pract.*, vol. 19, no. 7, pp. 658–674, Jul. 2011.
- [6] S. Simani, "Model-based fault diagnosis in dynamic systems using identification techniques," Universita degli Studi di Modena e Reggio Emilia, 2000.
- [7] Z. Gao, C. Cecati, and S. Ding, "A Survey of Fault Diagnosis and Fault-Tolerant Techniques Part I: Fault Diagnosis," *IEEE Trans. Ind. Electron.*, vol. 0046, no. c, pp. 1–1, 2015.
- [8] L. Liu and D. Cartes, "On-line identification and robust fault diagnosis for nonlinear PMSM drives," in *Proceedings of the American Control Conference*, 2005, pp. 2023–2027.
- [9] K. Rothenhagen and F. Fuchs, "Current sensor fault detection by bilinear observer for a doubly fed induction generator," in *32nd IEEE Annual Conference on Industrial Electronics*, 2006, pp. 1369–1374.
- [10] K. Rothenhagen, S. S. Member, and F. W. Fuchs, "Current Sensor Fault Detection , Isolation , and Reconfiguration for Doubly Fed Induction Generators," *IEEE Trans. Ind. Electron.*, vol. 56, no. 10, pp. 4239–4245, 2009.
- [11] K. Rothenhagen and F. W. Fuchs, "Doubly fed induction generator model-based sensor fault detection and control loop reconfiguration," *IEEE Trans. Ind. Electron.*, vol. 56, no. 10, pp. 4229–4238, 2009.
- [12] F. Grouz, L. Sbita, M. Boussak, and A. Khlaief, "FDI based on an adaptive observer for current and speed sensors of PMSM drives," *Simul. Model. Pract. Theory*, vol. 35, pp. 34–49, Jun. 2013.
- [13] T. A. Najafabadi, F. R. Salmasi, and P. Jabehdar-maralani, "Detection and Isolation of Speed-, DC-Link Voltage-, and Current-Sensor Faults Based on an Adaptive Observer in Induction-Motor Drives," *IEEE Trans. Ind. Electron.*, vol. 58, no. 5, pp. 1662–1672, 2011.
- [14] J. Gertler, "Fault detection and isolation using parity relations," *Control Eng. Pract.*, vol. 5, no. 5, pp. 653–661, May 1997.
- [15] B. H. Lee, N. J. Jeon, and H. C. Lee, "Current Sensor Fault Detection and Isolation of the driving motor for an In-wheel Motor Drive Vehicle," in *International Conference on Control, Automation and Systems*, 2011, pp. 486–491.
- [16] H. Berirri, M. W. Naouar, and I. Slama-Belkhodja, "Parity space approach for current sensor fault detection and isolation in electrical systems," *Eighth Int. Multi-Conference Syst. Signals Devices*, pp. 1–7, 2011.
- [17] H. Berirri, M. W. Naouar, and I. Slama-Belkhodja, "Easy and fast sensor fault detection and isolation algorithm for electrical drives," *IEEE Trans. Power Electron.*, vol. 27, no. 2, pp. 490–499, 2012.
- [18] M. Gálvez-Carrillo and M. Kinnaert, "A signal-based approach for detection and isolation of current sensor faults in induction motors," *Eur. Conf. Power Electron. Appl.*, pp. 1–10, 2009.
- [19] O. Touhami and M. Fadel, "Faults Diagnosis by Parameter Identification of the Squirrel Cage Induction Machine," *IEEE Int. Electr. Mach. Drives Conf.*, no. 1, pp. 821–825, 2007.
- [20] G. Stojcic and T. Wolbank, "Detection of defects in stator winding of inverter fed induction machines," in *IEEE International Electric Machines & Drives Conference*, 2013, pp. 111–116.
- [21] M. Gálvez-Carrillo and M. Kinnaert, "Sensor fault detection and isolation in doubly-fed induction generators accounting for parameter variations," *Renew. Energy*, vol. 36, no. 5, pp. 1447–1457, May 2011.
- [22] P. Vas, *Parameter Estimation, Condition Monitoring, and Diagnosis of Electrical Machines*. Clarendon Press, 1993.

## IX. BIOGRAPHIES

**Jon del Olmo** was born in Oiartzun, Spain in 1988. He received the B.S. degree in electronics engineering from the University of Mondragón, Mondragón, Spain, in 2012, where he is currently working toward the PhD. degree in the Department of Electronics, Faculty of Engineering. His current research interests include electric drives, fault detection and diagnostics.

**Javier Poza** was born in Bergara, Spain, in June 1975. He received the B.S. degree in electrical engineering from the University of Mondragón, Mondragón, Spain, in 1999, and the Ph.D. degree in electrical engineering from the INP, Grenoble, France. Since 2002, he has been with the Department of Electronics, Faculty of Engineering, University of Mondragón, where he is currently an Associate Professor. His current research interests include electrical machine design, modelling, and control. He has participated in various research projects in the fields of wind energy systems, lift drives, and railway traction.

**Txomin Nieva** was born in San Sebastian, Spain in 1972. He received a Computer Science Engineering degree in 1997 and a System Engineering degree in 1998 from the University of Mondragon, Spain, and a PhD in Computer Science from the EPFL, Switzerland, in 2001. Currently he is working as Technical Director of CAF P&A. His research areas are in power electronics in general and electrical traction systems in particular.

**Gaizka Ugalde** received the B.Eng. and Ph.D. degrees in electrical engineering from the University of Mondragón, Mondragón, Spain, in 2006 and 2009, respectively. Since 2009, he has been with the Department of Electronics, Faculty of Engineering, University of Mondragón, where he is currently an Associate Professor. His current research interests include permanent-magnet-machine design, modelling, and control. He has participated in various research projects in the fields of lift drives and railway traction.

**Leire Aldasoro** was born in a town near San Sebastian, Spain in 1981. She received the Industrial Engineering degree in 2005 from the University of Navarra (Tecnun). After working on the first traction system developed by CAF in its research and development area, currently she is the responsible of the Power Electronics Product Development group in CAF P&A. Her research area is electrical traction systems in general, focused on system's control algorithms.